DEVELOPMENT OF GAAS DETECTORS AT THE RWTH AACHEN [1]

Th. Kubicki, K. Lübelsmeyer, J. Ortmanns, M. Toporowsky, W. J. Xiao

I. Physikalisches Institut, RWTH Aachen
52056 Aachen, Germany [2]

ABSTRACT

Several GaAs surface barrier diodes with different areas have been fabricated and tested as particle detectors. To understand the behaviour of these detectors, a simple model of charge transport has been developed. Some of these detectors have been subjected to irradiation tests with different sources.

[1]presented at the 1st International Conference on Large Scale Applications and Radiation Hardness of Semiconductor Detectors, Florence, Italy, July 7th-9th, 1993

[2]This work was supported by the German Bundesministerium für Forschung und Technologie under contract number 056AC11P.

1 Introduction

The development of fast and radiation resistant detectors is an important requirement in view of high luminosity ($10^{33} - 10^{34}\,\mathrm{cm}^{-2}\mathrm{s}^{-1}$) pp-colliders like LHC. Inner tracking detectors and those used for photon localization inside an electromagnetic calorimeter have to withstand doses of 100Mrad or more and neutron fluencies in the range of $\Phi = 10^{14} - 10^{15}\,\frac{\mathrm{n}}{\mathrm{cm}^2}$ per year.
The great radiation resistance of devices made of GaAs and their successful application in high speed electronics (GaAs: $\mu_e \leq 8500\,\mathrm{cm}^2\mathrm{V}^{-1}\mathrm{s}^{-1}$, Si: $\mu_e \leq 1500\,\mathrm{cm}^2\mathrm{V}^{-1}\mathrm{s}^{-1}$) are well known [1]. GaAs is one of the most familiar materials of the III-V semiconductor compounds and is commercially easily available. So it is a very promising material for solid-state detectors that can be used at future proton colliders. The energy required to create an electron-hole pair in GaAs (4.2 eV) is nearly the same as in Si (3.6 eV) [2]. Because of the high Z (32) and density ($5.32\,\mathrm{gcm}^{-3}$), the radiation length of GaAs is $X_0 = 2.3\,\mathrm{cm}$ (Si: $X_0 = 9.36\,\mathrm{cm}$). Consequences are the higher multiple scattering and the higher probability of photon conversion but, considering the higher specific energy loss in GaAs ($\frac{\mathrm{dE}}{\mathrm{dx}} \sim 0.75\frac{\mathrm{keV}}{\mu\mathrm{m}}$ [3]) compared to Si ($\frac{\mathrm{dE}}{\mathrm{dx}} \sim 0.38\frac{\mathrm{keV}}{\mu\mathrm{m}}$ [4]), a 150μm thick GaAs-detector with 100 % charge collection efficiency will give roughly the same signal as a 300μm thick Si-detector.

2 The detectors

The GaAs wafers used for detector fabrication are standard 2″-wafers made of SI-GaAs. They were drawn by the LEC (Liquid Encapsulated Czrochalski) or VGF (Vertical Gradient Freeze) method. Table 1 shows the material properties of the GaAs-wafers used in this study [5] [6]. The main differences between LEC and VGF

Manufacturer:	Wacker	AXT
Crystal growth:	LEC	VGF
Diameter:	50.8 mm	50.8 mm
Orientation:	(100)	(100)
Doping:	Cr	undoped (EL2)
Thickness:	$350\,\mu$m	$450/350\,\mu$m
Resistivity:	$10^7 - 10^8\,\Omega$cm	$10^7 - 10^8\,\Omega$cm
Carrier conc.:	$10^7 - 10^8\,\mathrm{cm}^{-3}$	$10^7 - 10^8\,\mathrm{cm}^{-3}$
EPD:	$< 10^5\,\mathrm{cm}^{-2}$	$< 10^3/10^5\,\mathrm{cm}^{-2}$

Table 1: Relevant properties of the GaAs wafers as given by the manufacturer.

drawn material are the way to achieve compensation of shallow levels (caused by impurities) and the EPD:

- The shallow levels in the LEC material are compensated by a Cr-doping, in the VGF material by an antiside defect (EL2).

- The EPD in VGF material can be 2 orders of magnitude lower than in LEC material.

Fig. 1 shows the structure of 16 pad-detectors with two Schottky contacts (NiCr/Au). One Schottky contact covers the entire area of one side of the wafer. On the other

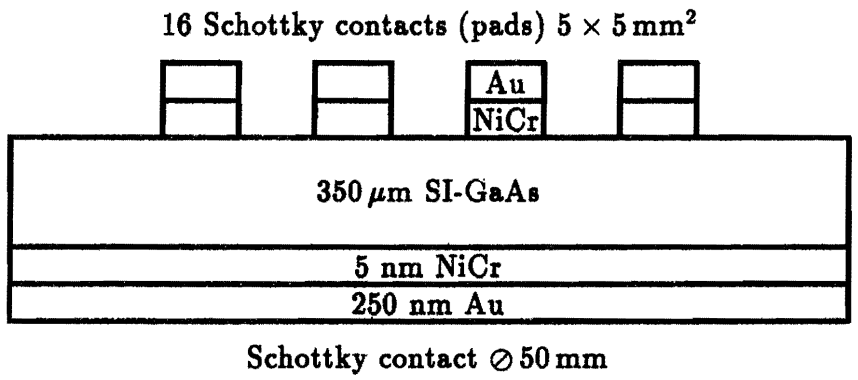

Figure 1: Structure of a 2″-GaAs-wafer with 16 pad-detectors. The entire backside of the wafer is covered by one Schottky contact.

side 16 Schottky contacts (pads) of an area of $5 \times 5\,\mathrm{mm}^2$ are prepared. The active area of the detectors is given by the area of the reverse biased Schottky contacts ($5 \times 5\,\mathrm{mm}^2$ pads). Effects of passivation and different surface treatments have also been studied [7].

2.1 Tests of electrical properties

The first step after fabrication is the test of electrical properties. All detectors show the expected I-V-characteristics. Given the MSM structure, the typical high diode current in the forward direction cannot occur: one of the Schottky contacts is always switched in the reverse direction. Fig. 2 shows typical I-V-characteristics (at room temperature) for 5 diodes (reverse biased pads). The current density in reverse direction is roughly $18\,\mathrm{nA/mm}^2$ at 100 V. The C-V-characteristics at frequencies higher than 1 kHz [3] [8] indicate that all detectors are fully depleted even at 0 V bias.

2.2 Charge collection efficiency of GaAs-detectors

To test the functionality of the diodes as detectors different sources are used, mainly ^{241}Am as an α/γ-source and ^{90}Sr to provide minimum ionizing electrons. The ^{241}Am-source is covered by a $\sim 1\,\mu\mathrm{m}$ window. The 5.5 MeV α-particles lose about 1.3 MeV

[3] The traps are not able to follow the test signal, and the capacitance is given by the movement of the electrons.

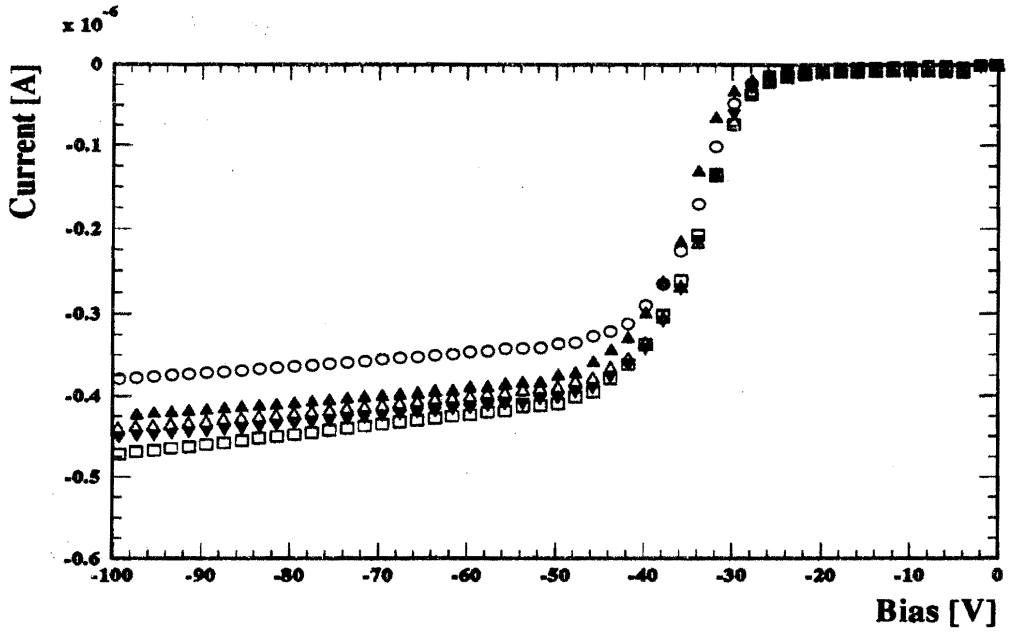

Figure 2: I-V-characteristics of $350\,\mu m$ thick undoped diodes without SiO_2-passivation. Schottky/Schottky contact: $5 \times 5\,mm^2$/ $\oslash 50\,mm$, EPD $< 10^3\,cm^{-2}$.

in this window and deposit the remaining energy completely in $10 - 15\,\mu m$ GaAs, producing $\sim 1 \cdot 10^6$ electron-hole pairs.

The calibration of the analog electronics including the ADC has been carried out using Si-detectors with 100 % charge collection efficiency and various sources in order to check the linearity of the ADC response to the deposited energy (created charge). The setup was evacuated to prevent energy loss of the α-particles in air. Fig. 3 shows an α-spectrum taken at 60 V bias voltage with the Si-detector. The α-peak appears at 4160 keV and corresponds to 100 % charge collection efficiency (ε_Q^α). The spectrum in Fig. 4 shows an α-spectrum taken with a GaAs-detector by irradiating the Schottky contact (signal due to drifting electrons) at 400V bias voltage. The α-peak has clearly shifted to lower energies (1870 keV) indicating that only part of the created charge has been collected. One finds a charge collection efficiency of

$$\varepsilon_Q^\alpha = \frac{\text{energy}_{\text{measured}}}{\text{energy}_{\text{deposited}}} = 45\,\%.$$

No signal is observed when irradiating the 'Ohmic' contact with α-particles (signal due to drifting holes).

Fig. 5 shows that the charge collection efficiency (ε_Q^α) for different detectors depends on the applied bias voltage U. It saturates for all types of detectors with the highest charge collection efficiency observed in detectors made of low EPD-material. It is interesting to note that these detectors show also the highest reverse currents.

Spectra of MIPs (minimum ionizing particles: here electrons) have been obtained using a ^{90}Sr-source with a plastic collimator (diameter: 3 mm) in front of the GaAs-detector and a Si-detector at the back of it whose signal is used to gate the ADC. A

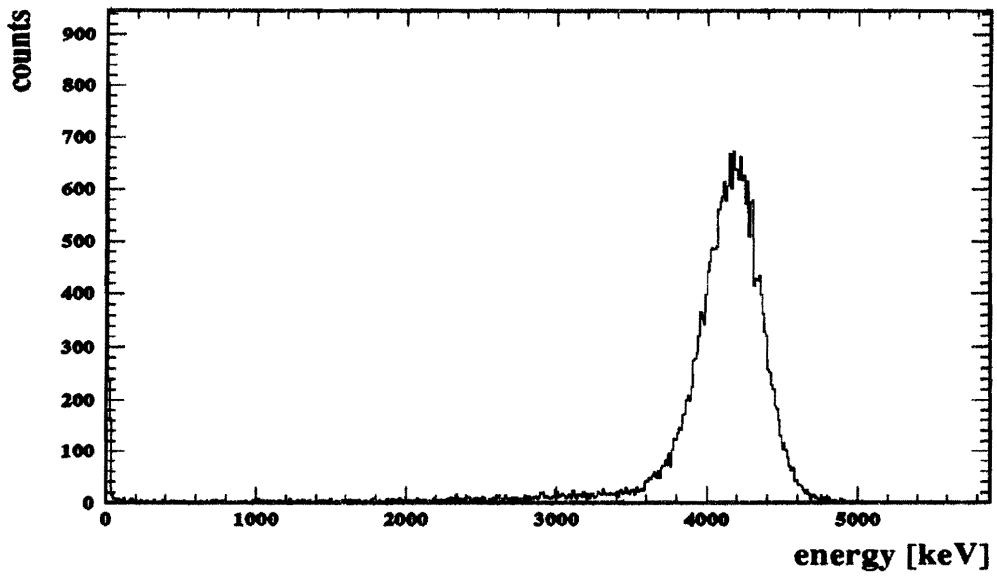

Figure 3: ^{241}Am α-spectrum taken with a Si-detector at 60 V, $\varepsilon_Q^\alpha = 100\,\%$.

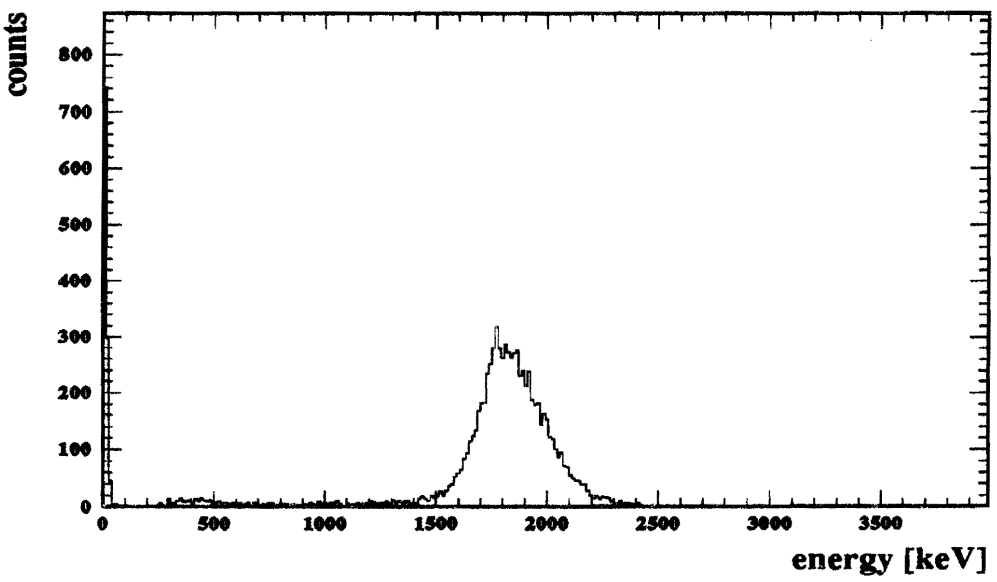

Figure 4: ^{241}Am α-spectrum taken with a 350 μm thick undoped GaAs-detector at 400 V. Schottky/Schottky contact: $5 \times 5\,\mathrm{mm}^2/\oslash\,50\,\mathrm{mm}$, EPD $< 10^3\,\mathrm{cm}^{-2}$.

thin sheet (3 mm) of plastic absorber was placed between the GaAs-detector and the Si-detector to ensure that only MIPs pass through the GaAs detector. We define the charge collection efficiency as the ratio of measured and calculated most probable

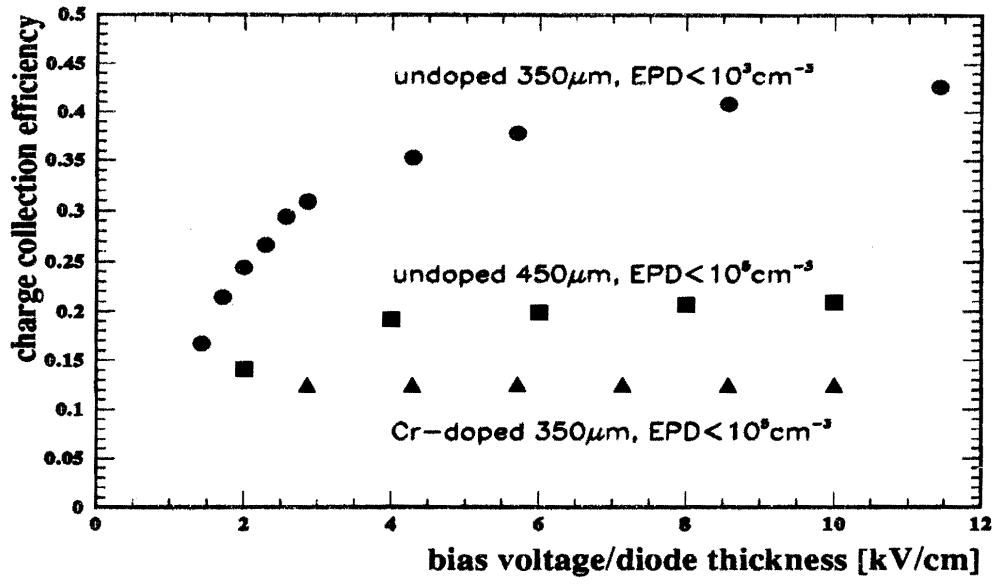

Figure 5: Charge collection efficiency ε_Q^α measured with α-particles for different GaAs-detectors.

(MOP) energy deposits:

$$\varepsilon_Q^{MIP} = \frac{MOP_{measured}}{MOP_{simulated}}$$

To calculate $MOP_{simulated}$ an optimized version [9] of the GEANT 3.14 program [10] was used. The simulation was checked replacing the GaAs-detector with a Si-detector. It can be seen from Fig. 6 that an excellent agreement between calculated and measured pulseheight spectra of ^{90}Sr-electrons in a Si-detector is achieved without introduction of any additional free parameters.
Calculated and measured pulseheight spectra of ^{90}Sr-electrons in a GaAs-detector are shown in Fig. 7. The difference between the MOP-values of the spectra is obvious and indicates the reduced charge collection efficiency for MIPs in GaAs. From the MOP-values one finds a charge collection efficiency of 42 % at 400 V bias voltage. As in the case of α-particles, the charge collection efficiency for MIPs also depends on the applied bias voltage. A nearly linear increase (Fig. 8) of charge collection efficiency with bias voltage is observed.

3 A simple model of charge transport

The behaviour of the detectors with regard to the reduced charge collection efficiency can be explained on the basis of trapping effects and the ionization of deep levels (Cr,EL2...) caused by band-bending .
The electric properties of the detectors can be described by solving the continuity-equation and the Poisson-equation [11] considering input parameters like donor-, acceptor-, trap-concentrations and trap energies. The ionization probability of deep

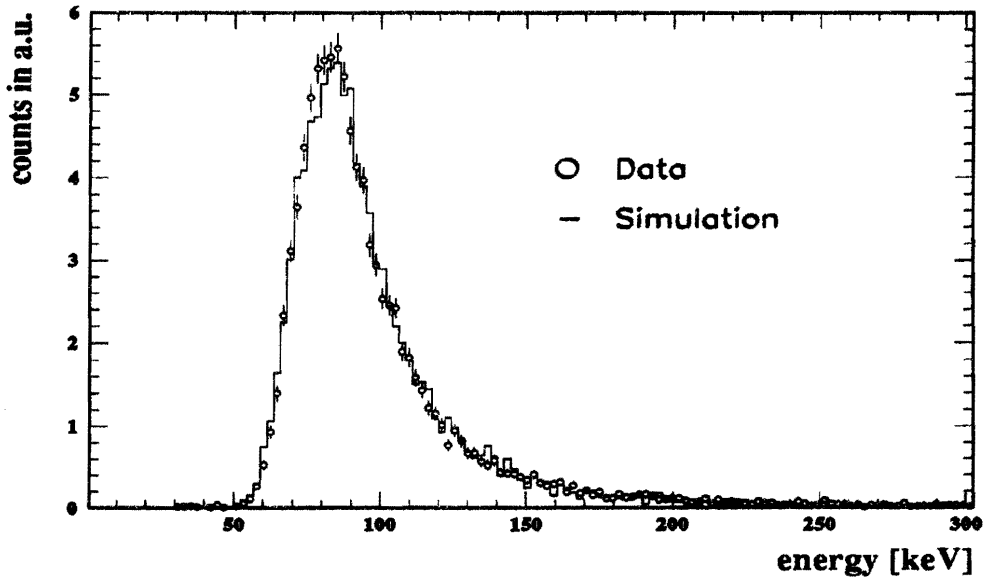

Figure 6: Measured ^{90}Sr MIP-spectrum taken at 100 V with a Si-detector (thickness: 300 μm) and GEANT 3.14 simulation, $\varepsilon_Q^{MIP} = 100\,\%$.

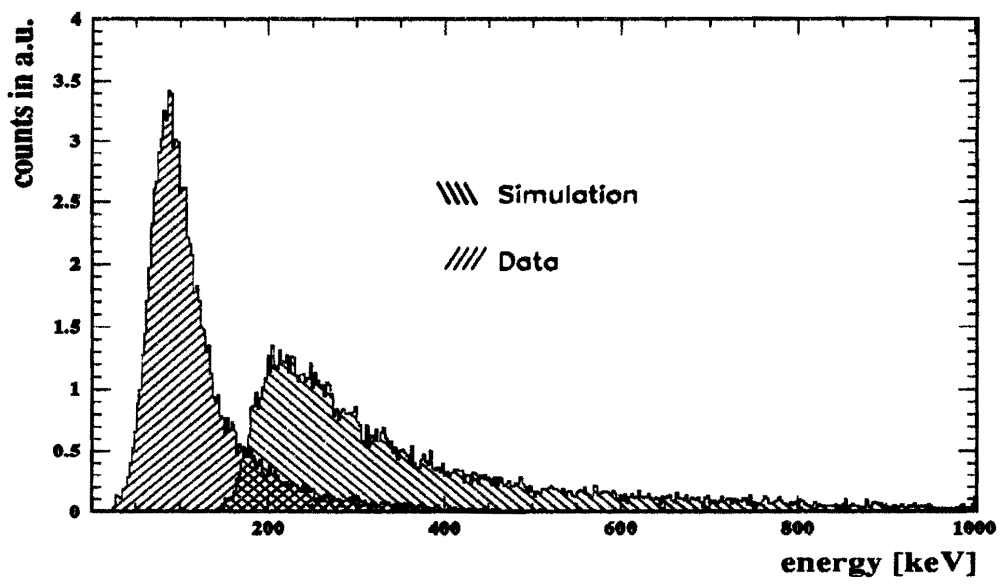

Figure 7: Measured ^{90}Sr MIP-spectrum taken with a 350 μm thick undoped GaAs-detector at 400 V and GEANT 3.14 simulation. Schottky/Schottky contact: $5 \times 5\,\mathrm{mm}^2/\oslash 50\,\mathrm{mm}$, EPD $< 10^3\,\mathrm{cm}^{-2}$, $\varepsilon_Q^{MIP} = 42\,\%$.

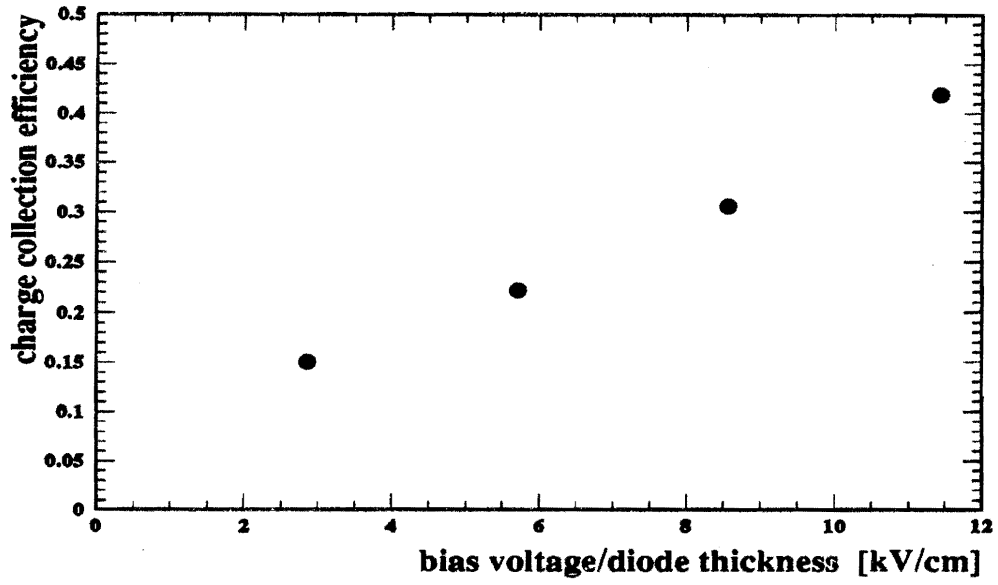

Figure 8: Charge collection efficiency ε_Q^{MIP} measured with minimum ionizing electrons for GaAs-detectors with EPD $< 10^3\,cm^{-2}$, $I_{rev} \sim 20\,nA/mm^2$.

levels is given by $e^{(\frac{E_F - E_T}{kT})}$ [12], where E_T denotes the energy of the deep levels and E_F the quasi-Fermi level [4]. Fig. 9a shows the calculated potential in a GaAs-detector (thickness: d=350μm) at 400 V reverse bias voltage. The difference $E_F - E_T$ across the detector is shown in Fig. 9b. In a domain close to the Schottky contact (up to roughly 270 μm from it) this difference is rather small ($< 0.2\,eV$). Consequently a considerable amount of deep levels can be ionized. At larger distances from the Schottky contact, $E_F - E_T$ is large and only few ionizations can occur. The corresponding space charge is plotted in Fig. 9c. A consequence of this nonuniform charge density distribution is an inhomogeneous electric field distribution (Fig. 9d).
The drift velocities for holes and electrons saturate already at comparably small fields [12] ($\sim 0.5 - 1\frac{V}{\mu m}$). This allows for the following model to describe the processes contributing to the charge transport in the detector: The detector (thickness d) is divided into an Active layer (high field region, thickness: X_A), where the drift velocities saturate and the mean free drift lengths for electrons and holes (λ_e^A, λ_h^A) are therefore taken to be constant, and a Dead (low field region) layer (Fig. 10) where the drift velocities and the mean free drift lengths (λ_e^D, λ_h^D) are field-dependent and are taken to be negligibly. We assume that ionizing particles create electron-hole pairs at the interaction point x_0 (see Fig. 10). The initial number of electrons and holes decreases exponentially as they move through the detector. Taking into ac-

[4]The quasi-Fermi level is a hypothetical energy level which is introduced to describe the behaviour of charge carriers under non-equilibrium conditions. It can be used in the same way as the Fermi level (in equations the Fermi level has to be replaced by the quasi-Fermi level) and correctly predicts the concentrations of the charge carriers in the corresponding bands if the carriers are assumed to be in thermal equilibrium [8].

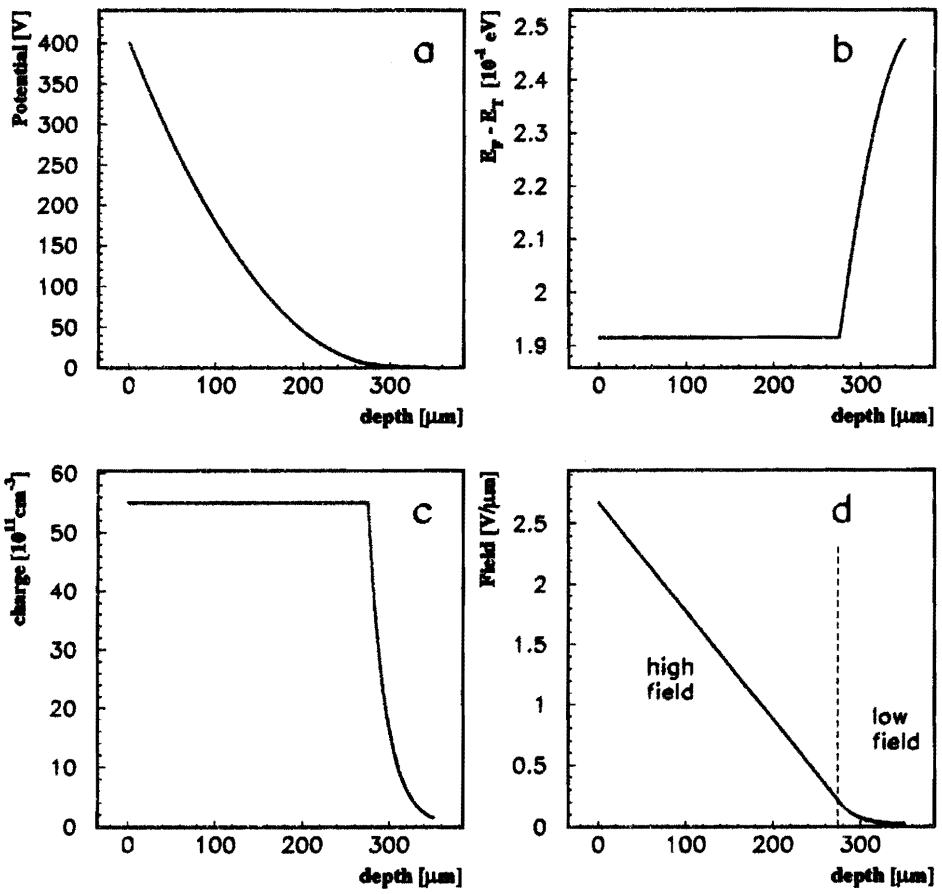

Figure 9: Distribution of a) potential, b) $E_F - E_T$, c) space charge density and d) electric field in a GaAs-detector (d=350 μm) with a Schottky contact.

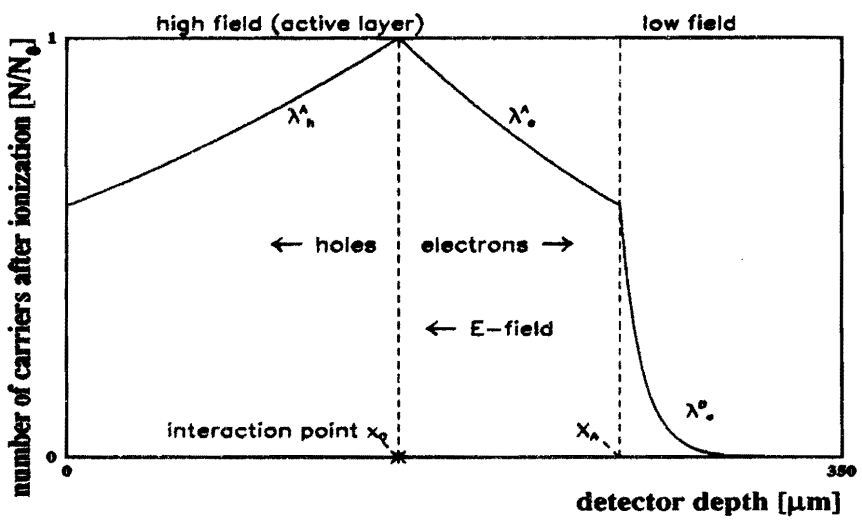

Figure 10: Number of drifting carriers versus detector coordinate in a GaAs-detector with a nonuniform field distribution and limited carrier lifetimes.

count Ramo's theorem [13] and the loss of drifting charge carriers, it is possible to calculate the charge collection efficiency.
In the case of α-particles penetrating the Schottky contact (signal only due to drifting electrons) we obtain for the charge collection efficiency:

$$\varepsilon_Q^\alpha = \frac{1}{d}\left[\int_0^{X_A} e^{-\frac{x}{\lambda_e^A}} dx + e^{-\frac{X_A}{\lambda_e^A}} \int_{X_A}^{d} e^{-\frac{(x-X_A)}{\lambda_e^D}} dx\right]$$

Parameters are the mean free drift lengths for electrons, the detector thickness and the thickness of the active layer. The results are shown in Fig. 11: plotted is the charge collection efficiency versus the thickness of the active layer for different values of the mean free drift lengths λ_e^A. Fig. 11 shows also four data points taken from

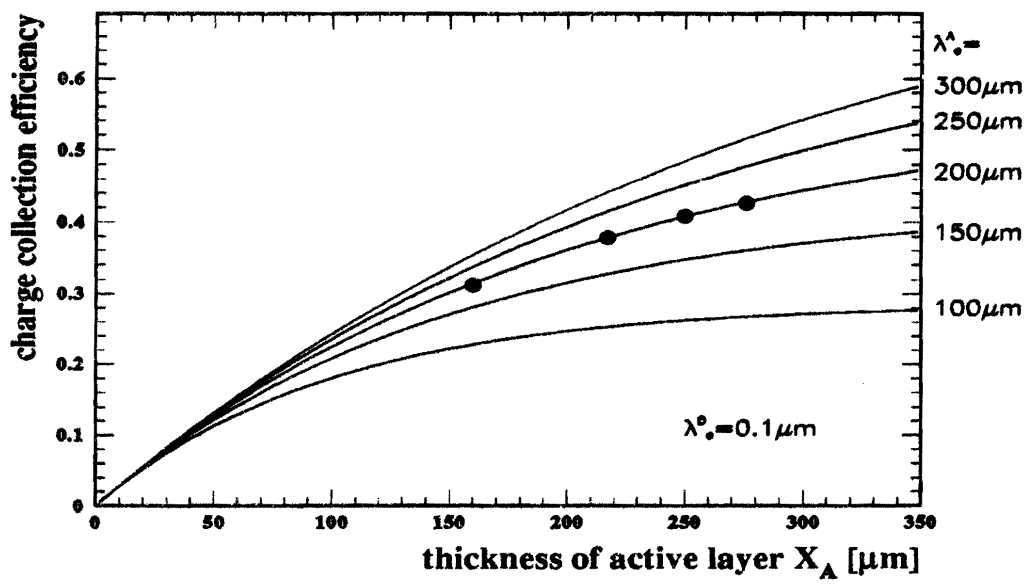

Figure 11: Charge collection efficiency versus thickness of the active layer for α-particles penetrating the Schottky contact. Parameters are the different mean free drift lengths for electrons, d = 350 μm.

Fig. 5 (those corresponding to the highest charge collection efficiencies for the undoped 350μm detector) assuming a reasonable mean free drift length $\lambda_e^A = 200\mu$m. The predicted correlation between active layer thickness X_A and applied bias voltage U is shown in Fig. 12. It is found to be linear, in agreement with the measurements of other groups [14], thus confirming the prediction by our model of the saturation effects shown in Fig. 5.
To compute the charge collection efficiency for minimum ionizing particles one first has to calculate the charge collection efficiency as a function of the interaction position x_0 within the detector taking into account the drift of electrons and holes.

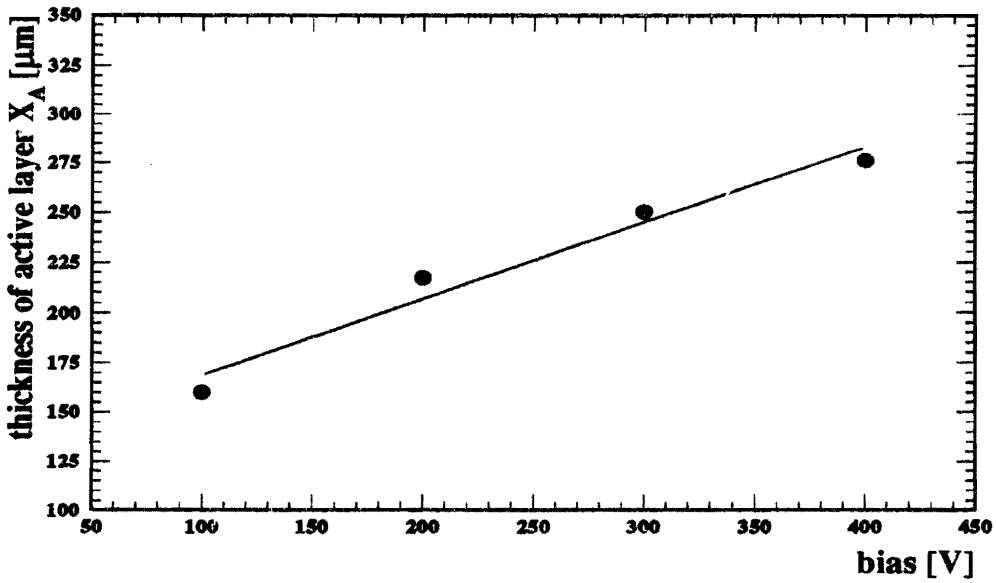

Figure 12: Active layer thickness X_A versus applied bias voltage U; the curve is a linear fit to the data.

Again using Ramo's theorem and the loss of drifting carriers one finds:

$$\begin{aligned} &\text{If } x_0 \leq X_A \\ \varepsilon_A(x_0, X_A, \lambda_i^j, d) &= \frac{1}{d}\Big[\int_0^{x_0} e^{-\frac{x_0-x}{\lambda_h^A}} dx + \\ &\quad + \int_{x_0}^{X_A} e^{-\frac{x-x_0}{\lambda_e^A}} dx + \\ &\quad + e^{-\frac{X_A-x_0}{\lambda_e^A}} \int_{X_A}^{d} e^{-\frac{x-X_A}{\lambda_e^D}} dx\Big] \qquad (1) \\ &\text{and if } x_0 > X_A \\ \varepsilon_D(x_0, X_A, \lambda_i^j, d) &= \frac{1}{d}[\cdots] \qquad (2) \end{aligned}$$

where λ_i^j denotes the different mean free drift lengths for electrons and holes in the different regions of the detector.
The charge collection efficiency of the entire detector (thickness d) for MIPs is given by

$$\varepsilon_Q^{MIP}(X_A, \lambda_i^j, d) = \int_0^{X_A} \varepsilon_A(x_0, X_A, \lambda_i^j, d)dx_0 + \int_{X_A}^{d} \varepsilon_D(x_0, X_A, \lambda_i^j, d)dx_0$$

Fig. 13 shows the charge collection efficiency for MIPs versus the thickness of the active layer for different mean free drift lengths of electrons and holes. Also shown are four measured data points (from Fig. 8) using the linear correlation between X_A and U from Fig. 12. For drift lengths of electrons and holes between 150μm and 200 μm

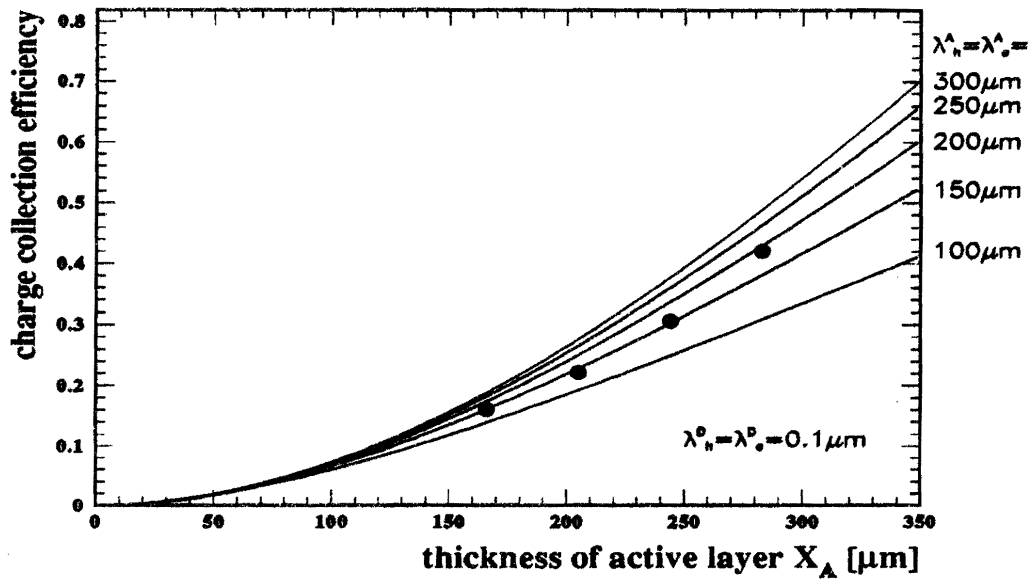

Figure 13: Charge collection efficiency versus thickness of the active layer for minimum ionizing particles. Parameters are the different mean free drift lengths for electrons and holes.

the data points follow the calculated curves, reproducing nicely the behaviour of charge collection efficiency ε_Q^{MIP} with increasing bias voltage. To improve the model, the position dependence of the electric field and the mean free drift lengths will be considered in future work.

4 Simulation of charge spectra

On the basis of the described model it is possible to simulate charge spectra of minimum ionizing electrons in GaAs using GEANT. The above described functions (eq. (1),(2)) which give the charge collection efficiency as a function of the interaction position, are used in an optimized [9] GEANT simulation. Each energy deposit is weighted with this functions depending on its position within the detector. Measured and calculated energy spectra of minimum ionizing electrons (^{90}Sr) in GaAs are shown in Fig. 14. The excellent agreement between data and simulation strongly supports our model of charge transport in GaAs.

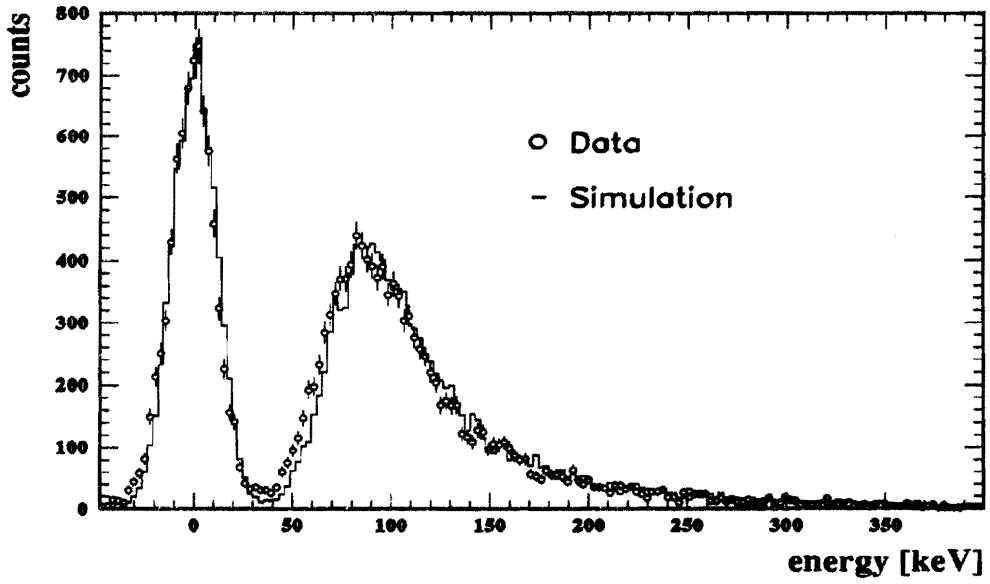

Figure 14: ^{90}Sr MIP-spectrum taken with a 350 μm thick undoped GaAs-detector at 400 V and a GEANT 3.14 simulation of this spectrum. Schottky/Schottky contact: $5 \times 5\,\mathrm{mm}^2/\oslash 50\,\mathrm{mm}$, EPD $< 10^3\,\mathrm{cm}^{-2}$. Parameters used are: $X_A = 270\,\mu\mathrm{m}$, $\sigma = 11.3\,\mathrm{KeV}$, $\lambda_e^A = \lambda_h^A = 200\,\mu\mathrm{m}$, $\lambda_e^D = \lambda_h^D = 0.1\,\mu\mathrm{m}$.

5 Tests of radiation hardness

We have performed several irradiation tests which have confirmed the radiation hardness of GaAs-detectors. The GaAs probes were irradiated with 3 MeV electrons and ^{60}Co photons up to a total dose of 100 Mrad [7] and with neutrons ($\Phi = 1.4 \cdot 10^{14}\,\mathrm{n/cm}^2$). The detector characteristics clearly deteriorated, but all detectors worked well after irradiation. More detailed tests of radiation hardness are in progress and will be published [15].

6 Conclusion

GaAs detectors have been fabricated and tested as particle detectors. They show a charge collection efficiency which can be interpreted in terms of a charge transport model based on trapping effects and the ionization of deep levels. Taking these effects into account simulated and measured charge spectra agree very well.

To further improve the understanding of the detector behaviour, studies with different detector structures (area, thickness) will be carried out. On one hand detector relevant properties like signal to noise ratio can be optimized. On the other hand important parameters like the mean free drift lengths for electrons and holes can be determined. A full simulation taking into account $\lambda(x)$, $E(x)$ will be the next step.

Further plans include:

- improvement of detector characteristics
- fabrication of microstrip detectors
- beam tests
- further tests of radiation hardness
- use of LPE/VPE-GaAs

Acknowledgements

We would like to thank K. Heime and A. Mesquida Küsters of IHT [5] and H. Vonhoegen for their support in detector fabrication. We also wish to thank E. Gerlach for several fruitful discussions.

[5] Institut für Halbleitertechnik Aachen

References

[1] C.T.Wang, Introduction to semiconductor technology, GaAs and related compounds, John Wiley & Sons, (1989), ISBN 0-471-63119-1

[2] M. Cuzin et al., Nucl. Instr. and Meth., A253 (1987) 407

[3] S. P. Beaumont et al., Nucl. Instr. and Meth., A326 (1993) 313

[4] Particle Data Group, Review of Particle Properties, Physical Review D11 (1992)

[5] Wacker-Chemitronic semiconductor materials product information

[6] American Xtal Technology product information

[7] W. Karpinski et al., Nucl. Instr. and Meth., A323 (1992) 635-637

[8] E. H. Rhoderick, R. H. Williams, Metal-Semiconductor Contacts, Clarendon Press Oxford (1988), ISBN 0-19-859336-8

[9] Th. Kubicki, Diploma thesis 1993, Aachen

[10] R. Brun et al., GEANT3 User's Guide, CERN DD/EE/84-1 (1986)

[11] W. J. Xiao, Phd. thesis in preparation

[12] S. M. Sze, Physics of Semiconductor Devices, John Wiley & Sons, New York (1983), ISBN O-471-O9837-X

[13] G. Cavalleri et al., Nucl. Instr. and Meth., 92 (1971), 137-140

[14] S. D'Auria, RD8 internal note, 1992

[15] O. Syben et al., Radiation Tests of GaAs-Detectors, PITHA 93/39 in preparation